Fast ion D-alpha measurements using a bandpass-filtered system on EAST

Zhang, J.; Huang, J.; Chang, J. F.; Wu, C. R.; Heidbrink, W. W.; Salewski, M.; Madsen, B.; Zhu, Y. B.; von Hellermann, M. G.; Gao, W.

Total number of authors:
12

Published in:
Review of Scientific Instruments

Link to article, DOI:
10.1063/1.5038828

Publication date:
2018

Document Version
Peer reviewed version

Fast ion D-alpha measurements using a bandpass-filtered system on EAST[a)]

J. Zhang,[1,2] J. Huang,[1] J. F. Chang,[1,b)] C. R. Wu,[1,2] W. W. Heidbrink,[3] M. Salewski,[4] B. Madsen,[4] Y. B. Zhu,[3] M.G. von Hellermann,[5] W. Gao,[1] Z. Xu,[6,7] and B. Wan[1]

[1)] *Institute of Plasma Physics, Chinese Academy of Sciences, P.O. 1126, 230031, Hefei, Anhui, China*

[2)] *University of Science and Technology of China, Hefei, Anhui 230026, China*

[3)] *Department of Physics and Astronomy, University of California Irvine, California 92697, USA*

[4)] *Department of Physics, Technical University of Denmark, Kgs. Lyngby, Denmark*

[5)] *FOM Institute DIFFER, Nieuwegein 3430 BE, Netherlands*

[6)] *Advanced Energy Research Center, Shenzhen University, Shenzhen 518060, Peoples Republic of China*

[7)] *Key Laboratory of Optoelectronic Devices and Systems of Ministry of Education and Guangdong Province, College of Optoelectronic Engineering, Shenzhen University, Shenzhen 518060, Peoples Republic of China*

(Dated: 13 July 2018)

Based on the charge exchange reaction between fast ions and a neutral beam, fast ion features can be inferred from the spectrum of Doppler-shifted Balmer-alpha light from energetic hydrogenic atoms. In order to study the interaction between instabilities and fast-ion transport, recently we extended the fast ion D-alpha (FIDA) measurements by using a combination of a band-pass filter and a photomultiplier tube (PMT) (f-FIDA). A band-pass filter selects the desired spectral band from 651 nm to 654 nm before detection by the PMT. Preliminary data from the EAST tokamak show that the active signals have been detected from reneutralized beam ions along the vertical and tangential viewing geometries. The details will be presented in this paper to primarily address the specifications and performance of f-FIDA hardware components and preliminary FIDA measurements.

I. INTRODUCTION

The research of fast ions in toroidal magnetic fusion devices becomes more important in recent years, because with the promotion of the plasma parameters and the heating methods, such as neutral beam injection (NBI) and ion cyclotron acceleration (ICRH), the fast ion product and its impacts on plasma become not negligible. Several diagnostics of fast ions have been developed on fusion devices. The fast-ion D-alpha diagnostic (FIDA)[1], first commissioned on DIII-D[2] in 2004 which is based on the charge exchange reaction between fast ions and a neutral beam, it is well known that fast ion features can be inferred from Doppler-shift of Balmer-alpha light from energetic hydrogen (deuterium) atoms. Then it has been applied on many magnetic devices[3–10].

To investigate the behavior of fast ions on EAST (Experimental Advanced Superconducting Tokamak), a FIDA diagnostic system with a spectrometer (s-FIDA)[11] was mounted since 2014 which is mainly used to analyze the different energy components of fast ions. In order to study the interaction between instabilities and fast-ion transport, recently the FIDA system was extended by using a combination of a band-pass filter and a photomultiplier tubes (PMT) (f-FIDA), which was first commissioned on NSTX[3] and also applied on DIII-D[4], and it will provide the temporal evolution of the blue shifted component of the Doppler shifted spectrum by integral the desired spectral band from 651nm to 654nm before detection by the PMT.

This paper is structured as follows. Sec. II introduces the current FIDA diagnostic layout on EAST. The instrument performance of the new f-FIDA systems including a comparison between multi-channel f-FIDA with array-PMT and single-PMT are shown in Sec. III. In Sec. IV, the application of FIDA in L-mode MHD quiescent plasmas is presented. Sec. V presents a summary.

II. FIDA DIAGNOSTIC LAYOUT

FIG. 1 shows the FIDA diagnostic layout on EAST[11]. The new f-FIDA systems are shown in the diagnostic room part of FIG. 1. EAST has both co-current (named as NBI1R,NBI1L) and counter-current (named as NBI2R, NBI2L) neutral beam injection (NBI). Each has two sources which can deliver 2-4 MW beam power with 50-80 keV beam energy as shown in EAST hall part of FIG. 1. Now, the diagnostic beam of the FIDA system is the beam of NBI1L. The active viewers including tangential and vertical viewers that intersect the NB, are towards the O horizontal and B vertical port and covering the region of major radii from 177 cm to 237 cm, and from 177 cm to 205 cm, respectively. The pas-

[a)] Published as part of the Proceedings of the 22nd Topical Conference on High-Temperature Plasma Diagnostics, San Diego, California, April, 2018.

[b)] Author to whom correspondence should be addressed. Electronic mail: changjiaf@ipp.ac.cn

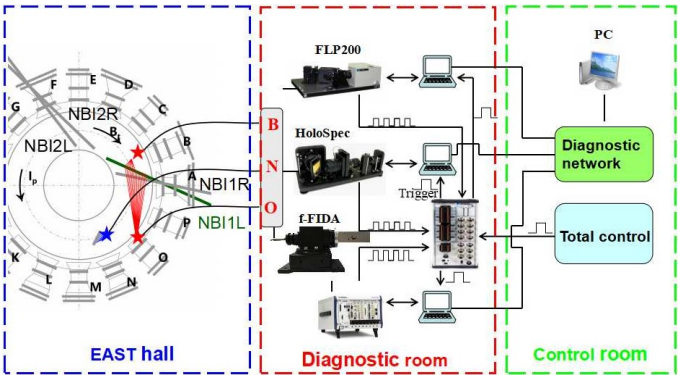

FIG. 1. (Color online). The FIDA diagnostic layout on EAST.

sive vertical N-port views that do not intersect a NB are geometrically the same as the active vertical B-port views. The optical fibers guide the signals to the FIDA instruments in the FIDA diagnostic room, keeping the detectors away from neutrons and gamma emission. Patch panels of the optical fiber link the fibers to the instruments allowing a flexible change of observation ports and instruments. To obtain good spectral resolution and high temporal resolution, respectively, high resolution spectrometers are equipped with both FLP200 and HoleSpec spectrometers[11], and fast filter-based photomultiplier systems including the array-PMT and single-PMT have been both available for the complementary measurements, respectively.

III. INSTRUMENT PERFORMANCE OF F-FIDA SYSTEMS

A. f-FIDA system with array-PMT.

The configuration of the f-FIDA system with an array-PMT is illustrated in FIG. 2. Light from EAST is collected by an eight-fiber array, and each fiber has 1500 μm core diameters and a numerical aperture of 0.37, the output spot of the fiber is 1.5 mm that is a surface light source. However, the input light has a certain divergence. The longer the focal length of the input lens, the smaller the divergence of the output light, but the larger the light spot. So when the optical fiber spot size is determined, the input lens is determined. The input lens (1) has a focal length of 10 mm, an outer diameter of 5 mm, its material is quartz, and the divergence angle at this time is 5 degrees. In order to make efficient use of the light energy and reduce cross-interference, the OD6 bandpass filters (2) with a center wavelength of 652.5 nm and a bandwidth of 3 nm should be as close as possible to the input lens. In the design, the filter position is placed at 25 mm from the input lens, then the output lens (3) with a focal length of 20 mm is placed at 25 mm from the filter, then the output lens focuses the light on the

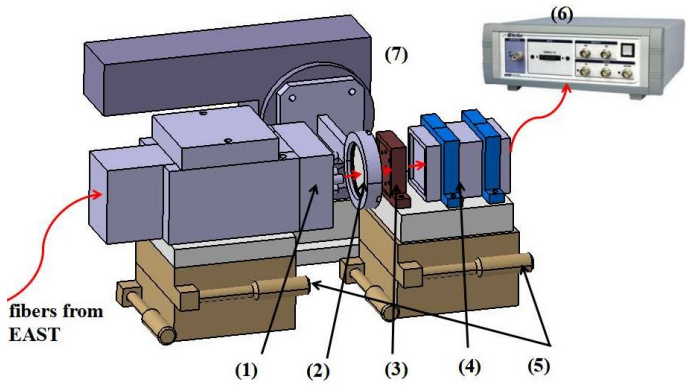

FIG. 2. (Color online). The schematic of the multi-channel f-FIDA with array-PMT. (1) Input lens; (2) Bandpass filters; (3) Output lens; (4) The photomultiplier tube (H8711-20); (5) Horizontal displacement stage; (6) The acquisition system (IQSP480); (7) Electric rotating table.

array-PMT (4). The image size of the fiber on the PMT cannot exceed 4 mm because the photosensitive surface of PMT detector is $4mm \times 4mm$. When the dimensions of the system parts are determined, the final image size on the PMT is 3 mm. The photomultiplier is a Hamamatsu tube, model H8711-20. If the received power is not enough, the distance between each part can be shortened by changing the horizontal displacement stage (5). At last, an acquisition system (6), a PhotoniQ IQSP480 from Vertilon Corporation, with maximum sampling rate up to 150 kHz transfers the data to a control PC. The center wavelength of the bandpass filters can change by rotating the electric rotating table (7) which is similar to that for single-PMT system and will be discussed later.

B. f-FIDA system with single-PMT.

The schematic of the f-FIDA system with multiple single-PMTs is shown in FIG. 3. Each of them consists

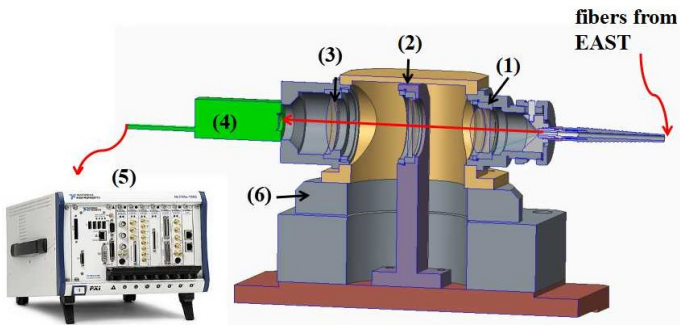

FIG. 3. (Color online). The schematic of the multi-channel f-FIDA with single-PMT. (1) Input lens; (2) Bandpass filters; (3) Output lens; (4) The photomultiplier tube (H10721-20) with the current amplifier; (5) The acquisition system (PXIe 1082 and NI PXIe-6368); (6) Rotary table.

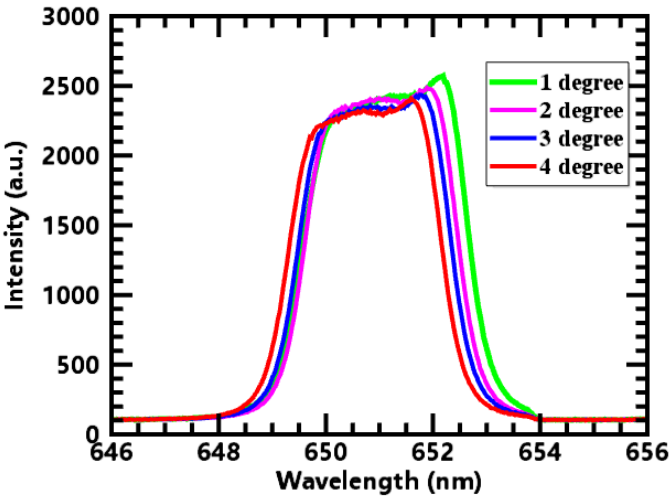

FIG. 4. (Color online). The measured transmittance curves with different angles between the filter and the optical path. The transmittance curve goes to the shorter wavelength direction when the angle between the filter and the light path is increased.

of two parts. The first part is the optical part. Light from EAST is collected by an optical fiber with a core diameter of 1500 μm and a numerical aperture of 0.37, then passes through the input lens (1) and focuses into parallel rays. The divergence angle at this time is 2 degrees. The input lens has a diameter of 25 mm and a focal length of 35 mm. Then the OD6 bandpass filters (2) select the desired passband with a center wavelength of 652.5 nm and a bandwidth of 3 nm.Then the output lens (3) which with a diameter of 29 mm and a focal length of 30 mm refocuses the light before reaching the PMT. The second part is the integrated part (4), which is mainly includes the photomultiplier tube using a Hamamatsu tube (model H10721-20), and the current amplifier. The optical signal of the PMT module is converted into a current signal which is finally converted into a voltage signal by a current amplifier with a bandwidth up to 500 kHz. At last, data is collected by an acquisition system (5), the acquisition box from National Instruments, is a NI Pxle-1082 and the acquisition card is NI Pxle-6368.The acquisition card has a bandwidth up to 250 MB/s, and its sampling rate reached 2 MHz. Under the premise of ensuring the collimation of the optical path, the focus is on the angle of the light incident on the filter, and the change of the transmittance curve of the filter due to this angle. By rotating the electric rotating table (6), the center wavelength of the bandpass filters can change which is measured by single-PMT as shown in FIG. 4. The transmittance curve goes to the shorter wavelength direction when the angle between the filter and the light path is increased. The center wavelength changes by 0.25nm for each 1 degree, and the result of clockwise rotation and counter clockwise rotation is the same.

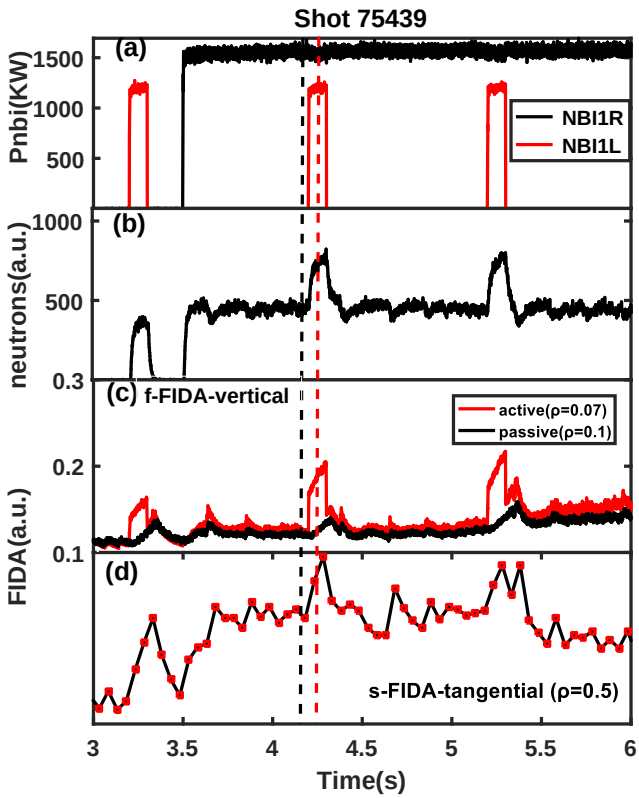

FIG. 5. (Color online). Time evolution of (a) the heating NBI source and the NBI1L is diagnostic beam, (b) the signal for neutrons, (c) the raw signals for vertical f-FIDA including active and passive, and (d) the integral signal for tangential s-FIDA between 651-654nm.

IV. PRELIMINARY MEASUREMENTS.

FIG. 5 shows waveforms of shot 75439 with $I_{\rm p}$~600 kA, $B_{\rm t}$~2.49 T. NBI1L and NBI1R are injected with beam energy of 55 keV and beam power of 1.2 MW and 1.5MW, respectively. The diagnostics beam NBI1L is injected for 100 ms and 10% duty, and the corresponding time periods for the three blips are 3.2-3.3 s, 4.2-4.3 s, 5.2-5.3 s as shown in FIG. 5(a). When the beams are turned on, the rate of neutrons increases rapidly and reaches its maximum value, where it remains until the beams is turned off as shown in FIG. 5(b).

There are two methods of background subtraction. One is beam modulation and the other is a paired passive view. FIG. 6 shows the typical measured spectrum data from the vertical view during beam-on (red dotted line in FIG. 5) and beam-off (black dotted line in FIG. 5) periods. The beam emission spectrum (BES) between 655-657 nm is strong during the beam-on phase[12]. The beam emission, D_α light from halo neutrals and the cold D_α line have been eliminated by an OD3 neutral density filter, and visible bremsstrahlung is a nearly flat spectral feature in this wavelength band. There are few impurity line emissions such as OV at 650nm presents in

the blue-shifted wing of the cold D_α line. Thus a bandpass filter selects the 651-654nm range for the application of f-FIDA which avoids the bright sources of light and impurity lines. The background signal is the same in the beam-on and beam-off periods, as it does not arise from charge exchange and it does not contribute to the measured fast-ion signal. This shows that the plasma is in steady-state. By background subtraction approaches, passive FIDA radiation can be eliminated to obtain net FIDA spectra (green line in FIG. 6). The passive oxygen lines disappear completely.

FIG. 5(d) is calculated by integrating the tangential view of s-FIDA spectra signals between 651-654 nm wavelengths. The exposure time of s-FIDA is 20 ms to ensure that there are two frames in one blip of the NBIs. A clear increase is observed for the beam-on phase and reduction for the beam-off phase, but sometimes when the neutral beam is turned off, the integrated intensity continues to rise, and this is because of the increased background signal of bremsstrahlung.

FIG. 5(c) shows the time evolution of two vertical f-FIDA views. One is the vertical active at R∼1.90 m and ∼0.07 from B-port viewing the diagnostic beam, the other one is the vertical passive at R∼1.92 m and ∼0.10 from N-port. The f-FIDA signals come from two sources: an active component from charge exchange with the injected beam and a passive component from charge exchange with edge neutrals and visible bremsstrahlung. The active component is only there when the beam is on and the passive component is there whether the beam is on or off. When the diagnostic beam NBI1L is on, the f-FIDA signal with the active view rises and then when the beam turns off there is a rapid drop. During each blip the active signal should rise as the number of beam ions builds up. The rise depends on the absolute intensity calibration. In contrast, the decay time analysis is independent of the absolute calibration of the f-FIDA diagnostic. The expected behavior of the active signal has features similar to the behavior of the neutron emission, but the rate of neutrons increases rapidly and reaches its

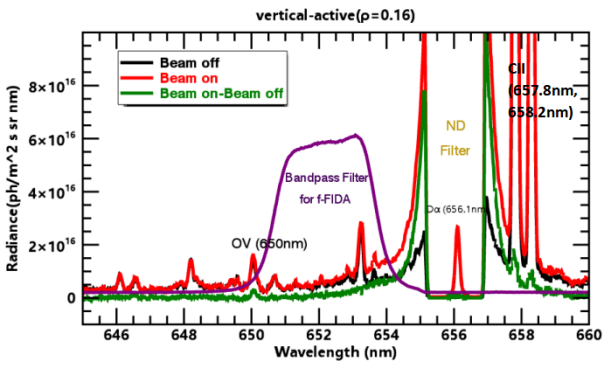

FIG. 6. (Color online). Measurement of beam-on (4.25 s), beam-off (4.19 s) spectra and a transmittance curve of filter on s-FIDA diagnostic system.

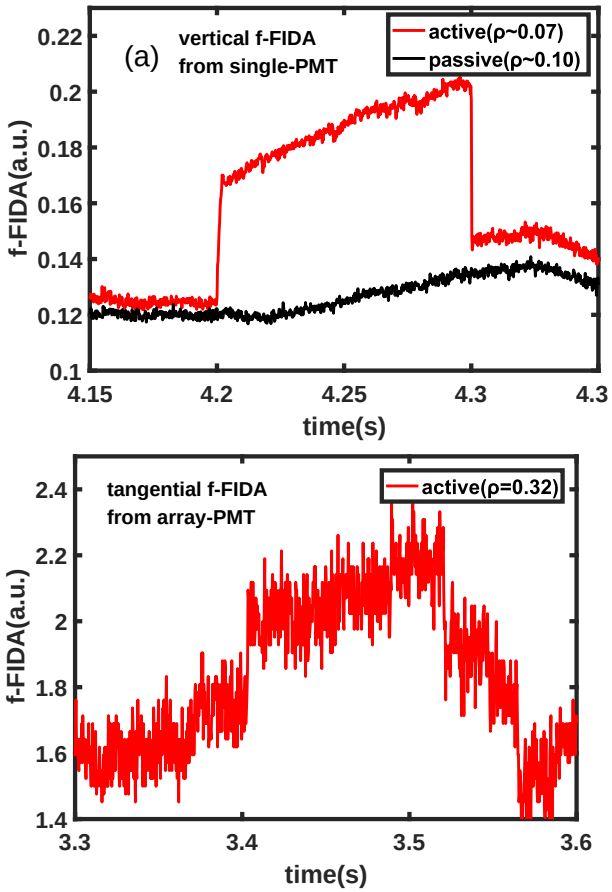

FIG. 7. (Color online).(a) Details of the f-FIDA signals in FIG. 5(c) between the time ranges of the second blip of NBI1L in discharge 75439. (b) The active f-FIDA signal of the multi-channel f-FIDA with array-PMT in discharge 71695.

maximum value in about 0.1 s and the active signal is more rapid. The expected rise of the waveform is different for passive f-FIDA than for the neutrons because the weight function has a different energy and pitch dependence actually. This work of passive FIDA have been applied on DIII-D[13] and NSTX[14]. The details will be further investigated.

FIG. 7 shows the comparison f-FIDA signals between two sets of f-FIDA with single-PMT and array-PMT systems. FIG. 7(a) is the zoom of second of NBI1L shown in FIG. 5(c). FIG. 7(b) is the raw active f-FIDA data from the array-PMT at R∼1.75 m and ∼0.32 from O-port viewing in discharge 71695. EAST plasma data: I_p∼400 kA, B_t∼2.5 T, co-current (NBI1L) and counter-current (NBI2R) neutral beams are injected with beam voltage of 55keV and time period for the second blip of NBI1L is 3.47-3.57s. Although the onset of the f-FIDA shows a jump in the active signal due to the injected neutral beam, the array-PMT f-FIDA system has worse signal to noise ratio compared with the single-PMT.

Two f-FIDA systems are currently available, and single-PMT is preferred due to high transmittance, sam-

pling rate and depth of parallelism. First, after testing, the optical power entering the array-PMT is 15mW, and the converged optical power is 9mW, so the optical utilization of the array-PMT is 60%. The same method measures the optical utilization of the single-PMT to 90%. The change of the light utilization depends on the size of the entire system, because the size of the array-PMT is fixed and the single-PMT is flexible, mainly depending on the change in the focal length and diameter of the lens. Furthermore, the difference in sampling rates depends on the different acquisition systems. The maximum trigger frequency of the array-PMT is 150 kHz and the single-PMT is 2 MHz. Last, due to limited device size of array-PMT, the divergence angle is 5 degrees, but the single-PMT is more flexible which has a bigger lens and a longer focal length, so the depth of parallelism of single-PMT is better than for the array-PMT.

V. SUMMARY.

To obtain high temporal resolution for FIDA diagnostics, fast filter-based photomultiplier systems have been developed on EAST which can supply the complementary measurements to previous s-FIDA with good spectral resolution measured by high resolution spectrometers. Two sets of f-FIDA with array-PMT and single-PMT and will be applied to study the impact of MHD modes and energetic particle instabilities on fast-ion transport for high performance long pulse discharges on EAST.

ACKNOWLEDGMENTS

This is supported by Natural Science Foundation of China Grant No. 11575249, National Magnetic Confinement Fusion Energy Research Program under Grant Nos. 2015GB110005, 2014GB109004 and Hefei Science Center CAS (2017HSC-IU005).

[1]W. W. Heidbrink, Rev. Sci. Instrum. **81**, 10D727 (2010).
[2]W. W. Heidbrink *et al.*, Plasma Phys. Control. Fusion **46**, 1885 (2004).
[3]M. Podestà *et al.*, Rev. Sci. Instrum. **79**, 10E521 (2008).
[4]C. M. Muscatello *et al.*, Rev. Sci. Instrum. **81**, 10D316 (2010).
[5]M Salewski *et al.*, Nuclear Fusion **54**, 023005 (2014).
[6]M. Osakabe *et al.*, Rev. Sci. Instrum. **79**, 10E519 (2008).
[7]B. Geiger *et al.*, Plasma Phys. Control. Fusion **53**, 065010 (2011).
[8]C. Michael *et al.*, Plasma Phys. Control. Fusion **55**, 095007 (2013).
[9]J. Huang *et al.*, Rev. Sci. Instrum. **85**, 11E407 (2014).
[10]B. Geiger *et al.*, Plasma Phys. Control. Fusion **59**, 115002 (2017).
[11]Y. M. Hou *et al.*, Rev. Sci. Instrum. **87**, 11E552 (2016).
[12]J. Huang *et al.*, Rev. Sci. Instrum. **87**, 11E542 (2016).
[13]Nathan G. Bolte *et al.*, Nucl. Fusion. **56**, 112023 (2016).
[14]G.Z.Hao *et al.*, Plasma Phys. Control. Fusion. **60**, 025026 (2018).